Effects of Freeze-Thaw and Photobleaching on the Ultraviolet Resonance Raman Spectra of Human Colon Biopsies

NADA N. BOUSTANY,* JAMES M. CRAWFORD, RAMASAMY MANOHARAN, RAMACHANDRA R. DASARI, and MICHAEL S. FELD

George R. Harrisson Spectroscopy Laboratory, Massachusetts Institute of Technology, Cambridge, Massachusetts 02139 (N.N.B., R.R.D., M.S.F.); Harvard-MIT Division of Health Sciences and Technology, Massachusetts Institute of Technology, Cambridge, Massachusetts 02139 (N.N.B); Department of Pathology, Immunology and Laboratory Medicine, University of Florida College of Medicine, Gainesville, Florida 32610 (J.M.C.); and Rosemount Analytical Inc., Orrville, Ohio, 44691 (R.M.)

We studied the effects of sample freezing and thawing, laser fluence, temperature, and oxygen on the ultraviolet resonance Raman (UVRR) spectra of human colon biopsies at 251 nm excitation. We show that the total adenylate content of the tissue decreases as a result of freezing and subsequent thawing to room temperature. We also show that photobleaching is the result of oxidative as well as thermal damage. Photobleaching consisted of a decrease in the intensity of the purine spectral bands and broadening and intensity increase of the aromatic amino acid bands. Both bio- and photodegradation of the tissue can be minimized by keeping the biopsy samples refrigerated during testing and the laser fluence under 0.2 mJ/μm^2. Unlike amino acid photobleaching, purine photobleaching was also greatly reduced by placing the samples in an argon atmosphere. Sample storage could be achieved by refrigerating the fresh specimens and testing them within 30 h of surgical resection, without freezing. Alternatively, the fresh specimens could be snap-frozen in liquid nitrogen, then thawed and tested for up to 30 min. Altogether, these studies can be utilized to guide future experimental design and data interpretation during ultraviolet spectroscopy of biological tissues.

Index Headings: **Ultraviolet resonance Raman spectroscopy; Human colon; Photobleaching; Purine photodamage; Tryptophan and tyrosine photodamage; Cryopreservation.**

INTRODUCTION

Recently, we and others have published ultraviolet resonance Raman (UVRR) spectroscopy studies of normal and neoplastic tissues with 251 and 257 nm excitation.[1–3] Those studies show how combined bulk and microscopic UVRR spectroscopy of biological tissues can potentially provide a new tool for tissue bioassay, pathological analysis, and histochemistry. However, the quality and reproducibility of the UVRR spectra to be eventually collected from human biopsies will likely depend on the freeze/thaw history of the tissue and the UV energy dose (fluence) delivered at the sample surface. Around 250 nm excitation, the resonantly enhanced molecules in biological tissue are mainly nucleic acids, nucleotides, and the aromatic amino acids tryptophan and tyrosine, which are found in peptides and proteins. The nucleic acids and nucleotides have absorption peaks near 260 nm; the aromatic amino acids, near 280 and 220 nm. When excited by ultraviolet light between 200 and 300 nm, all of these molecules are known to undergo photochemical changes and form a variety of photoproducts. In addition, these tissue biochemicals are potentially labile and may be affected by freezing and thawing.

In this paper we describe the spectral artifacts observed during UVRR spectroscopy of human colon tissue and the methods used to avoid them and collect reproducible data. We measured the effects of fluence, temperature, and oxygen on photobleaching. With respect to biochemical degradation, experiments were designed to answer the following questions: ''How stable is the UVRR spectrum over the testing period?'', ''Does freezing and thawing affect the spectral line shape?'', and ''How long after surgical resection can the sample be kept and still yield reproducible data?''

While UVRR spectroscopy studies of biological tissue are often concerned with collecting spectra with adequate signal-to-noise ratios, our studies show that additional parameters, such as photochemical and biochemical tissue damage, can greatly affect the quality of the UVRR spectra collected from biological tissue. By calling attention to these biochemical and photochemical effects, and by proposing methods to minimize them, these studies can serve as a guide for future experimental design and data interpretation during ultraviolet spectroscopy of biological tissues.

METHODS

Apparatus. The UVRR system, which was used to collect the spectra, was described previously.[3] Briefly, our excitation source uses the third harmonic of a tunable, argon laser pumped, mode-locked Ti : sapphire laser (Coherent Inc.). The laser excitation wavelength was tuned to 251 nm. This quasi-continuous laser system produces 2–3 ps pulses at 76 MHz. The collected Raman-scattered light is launched into a 1-m-long f/8 spectrometer (SPEX/Jobin-Yvon) that disperses it at 0.4 nm/mm with a single 2400 grooves/mm grating across a liquid nitrogen cooled charge-coupled-device (CCD) detector (Princeton Instruments). A spectrometer entrance slit of 150 μm produced a spectrometer resolution of 9 cm^{-1} (0.06 nm), but the overall system resolution was limited to 15 cm^{-1} by the laser bandwidth. This resolution is adequate for Raman studies of biological tissue, which has Raman bands ~30 cm^{-1} wide. A dielectric longpass filter (Barr Associates,

Received 30 April 2001; accepted 16 July 2001.

* Author to whom correspondence should be sent. Current address: Johns Hopkins University School of Medicine, Biomedical Engineering Department, 720 Rutland Ave, Traylor 701, Baltimore, MD 21205.

0003-7028/01/5511-1506$2.00/0

TABLE I. List of samples tested from each patient in the different conditions. Sample numbers are written in the form *x.y*, where *x* denotes the patient number, and *y* the sample number from that patient.

Patients	1	2	3	4	5
Free-thaw					
Condition 1: Freeze-thaw to room temperature		2.1		4.4	5.3
Condition 1: Freeze-thaw to 0–4 °C			3.1	4.2	
Condition 2: 0–4 °C, No freezing				4.1, 4.2, 4.3	5.1, 5.2
Condition 3: Test before and after freezing				4.2	
Photobleaching					
Air—room temperature	1.1, 1.2		3.2		
Air—2–3 °C					5.4
Argon—room temperature			3.3, 3.4, 3.5		

Westford MA) or liquid solution filter was placed in the light-scattering optical collection path to reject the Rayleigh scattered light. The solution was prepared from a stock containing 2.5×10^{-5} M anthracene and 0.5 M KI dissolved in ethanol : water (1:1::V:V). The stock was subsequently diluted 13 times in pure ethanol and placed in a 1-cm-pathlength quartz cuvette. The filter solution was renewed before every experimental run, and its absorption spectrum was measured and found to be consistent before and after each run, as well as from day to day. Spectra of ethanol and acetone were collected to calibrate the Raman-shift axis in the wavenumber range 1000–1800 cm^{-1}. Utilizing the known Raman band positions of ethanol and acetone,[4–5] a third-order polynomial interpolation was used to convert CCD pixel numbers to wavenumbers.[6] The spectra were not intensity calibrated since this calibration was not necessary for our studies, in which we compare relative changes between spectra. The intensity (in arbitrary units) of the reported spectra (Figs. 1 and 5) represents the raw signal collected from the CCD detector at each wavenumber.

We used human colon specimens for our studies. For each condition tested, the number of samples and patients from which the samples were collected are summarized in Table I. During spectroscopy, the samples were placed in a standard cuvette containing phosphate buffered saline (pH = 7.4). When needed, the cuvette was refrigerated to 0–4 °C with thermo-electric coolers (model CP 1.0-17-05L, Melcor Thermoelectrics, Trenton, NJ). The colon sample was positioned in the cuvette with the mucosa facing the incident beam. The Raman-scattered light was collected in an epi-illumination geometry. The excitation laser beam impinged on the cuvette surface at an ~60° angle to the optical axis, defined by the spectrometer, to avoid collecting specular reflection of the laser light. The incident laser beam gave a spot area of 35 μm × 40 μm. A neutral density filter was placed in the excitation path to reduce the power striking the tissue to ~2–5 mW.

Freeze-Thaw Study Protocols. Samples of normal human colon tissue were obtained after surgical resection. Partial colectomy specimens were resected from patients with colonic cancer. Within 10 min of receipt from the operating room, 1 cm × 1 cm full-thickness samples of normal colonic tissue at least 3 cm from the colon cancer were prepared by scalpel incision. These samples consisted of normal colonic mucosa, submucosa, muscle wall, and serosa. The fresh samples were stored and tested under three different conditions (Table I):

Condition 1: Five of the fresh samples were snap-frozen in liquid nitrogen, stored at −80 °C, and tested after thawing. Spectroscopy was done at either room temperature or 0–4 °C.

Condition 2: Five samples from two different patients were kept fresh in refrigerated phosphate buffered saline (pH = 7.4), without freezing, and tested at periodic intervals after the surgical resection.

Condition 3: One fresh sample was tested before freezing. The same specimen was then snap-frozen in liquid nitrogen and tested again immediately after thawing to 0–4 °C.

Conditions 1 and 3 were designed to study the stability of the UVRR spectra and the effects of freezing and thawing on the UVRR spectra, while Condition 2 was designed to investigate spectral changes that may occur once the tissue is removed from the body.

In these freeze-thaw studies, the power striking the tissue was ~2–3 mW. Given the measured laser spot size at the sample (35 μm × 40 μm), this results in an intensity of I = 1.4–2.1 μW/μm^2 at the sample. The tissue sample holder was mounted on a translational stage, and the stage actuator was connected to a 4-rotations-per-minute AC motor to move the sample across the incident beam at ~2 mm/min. This movement minimized laser exposure time on an individual spot (~1.5 s/spot). A 3.3-mm strip along the tissue surface was scanned by the laser during a typical signal collection time of 100 s. Each colon specimen was scanned over most of its surface by collecting ~10–30 spectra as the laser beam was translated back and forth in a repeating S-shaped pattern down the sample surface. A new excitation pattern was traced for each spectrum.

The spectral contributions of adenosine and guanosine were calculated from a linear spectral model of the UVRR line shape. As described previously,[2] the spectra were modeled by a linear combination of 10 line shapes consisting of AMP, FAD, GMP, CMP, TMP, UMP, tryptophan, tyrosine, lipid, and water, using a least-squares minimization algorithm. The level of adenosine relative to guanosine was plotted as the ratio of the sum of the AMP and FAD fit parameters to the GMP fit parameter, or $(a_{AMP} + a_{FAD})/a_{GMP}$. The level of guanosine was plotted separately as the GMP fit parameter, a_{GMP}.

Photobleaching Protocols. In these studies, the normal colon tissue obtained from surgical resections was immediately snap-frozen in liquid nitrogen and stored at −80 °C until use. Bulk specimens were prepared by thawing the tissue in phosphate buffered saline (pH =

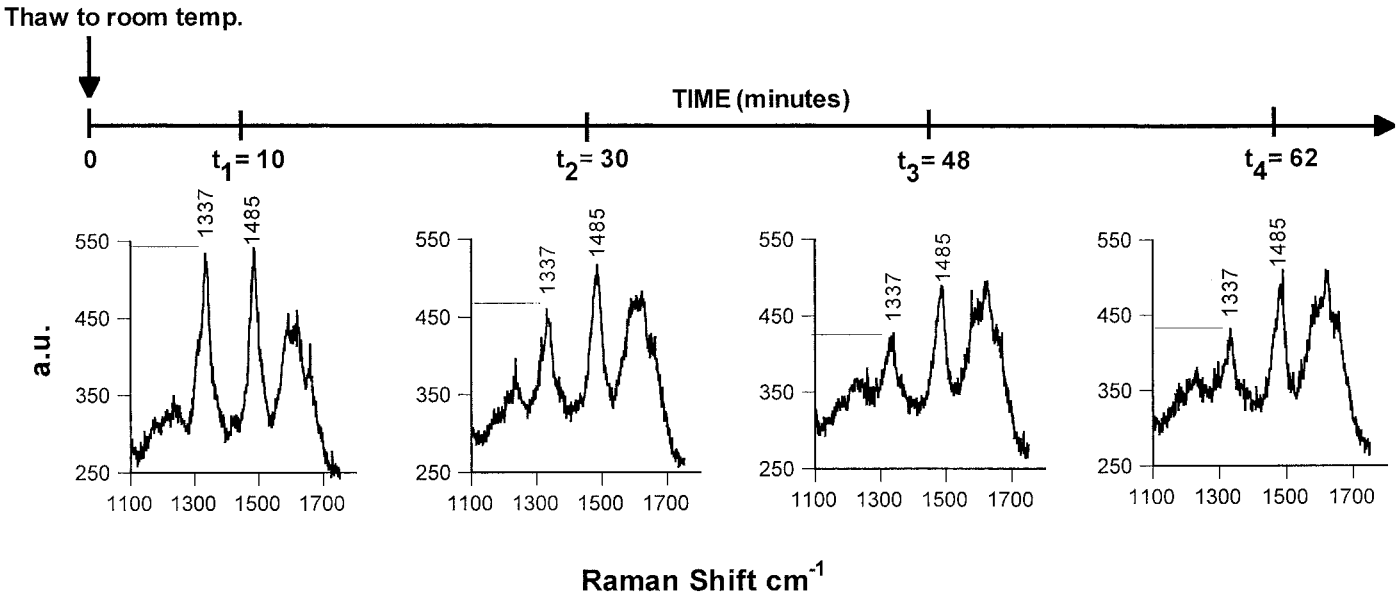

FIG. 1. Spectral changes due to specimen freezing and thawing. UVRR spectra of colon were collected from colon samples immediately after thawing to room temperature. After 10 min of data acquisition, the signals at 1337 and 1485 cm^{-1} decreased dramatically and seemed to correspond to a decrease in adenosine. The time bar indicates the time at which each spectrum shown was collected after thawing. Time t = 0 represents the moment the sample reached room temperature, as measured by a thermocouple near the mucosal surface. **a.u.** = arbitrary units representing the raw signal intensity collected from the CCD detector.

7.4) and selecting mucosal locations for spectroscopic examination. The spectra were acquired from mucosal locations on stationary bulk tissue samples (in contrast to the freeze-thaw study, in which the samples were translated across the excitation beam). The laser power at the sample was kept between 2 and 5 mW. The laser fluence was varied by varying the exposure time while keeping the power constant within each study. Several mucosal locations were analyzed on each bulk sample. To prevent spectral changes due to freezing and thawing from affecting the photobleaching studies, specimens were kept at room temperature for ~30 min to wait for the adenosine signal to reach its minimal value (see results, Fig. 1).

Temperature effects on photobleaching were investigated by testing the samples at either room temperature or at 0–4 °C. The effect of oxygen on photochemical degradation was investigated by measuring spectra of bulk colon tissue samples at room temperature in an argon atmosphere. For the argon studies, samples were placed in a cuvette through which argon flowed via ports in the cuvette cover. An argon atmosphere bathed each sample for ~45 min before spectroscopy studies started. To avoid sample dehydration, the argon was diffused through water. Table I details the samples used in each condition.

Photobleaching was quantified by monitoring the intensity of the purine Raman band centered at 1485 cm^{-1} as a function of laser energy. Collected spectra were fit in the range between 1450 cm^{-1} and 1550 cm^{-1} to the GMP line shape and a constant background by least-squares minimization (LSM). The LSM weighting parameter for GMP is indicative of the area under the 1485 cm^{-1} peak after background subtraction. Instead of simply integrating under the band, this LSM fitting technique was used to improve background signal subtraction. The 1485 cm^{-1} peak has a contribution from adenosine as well as guanosine, and both of these compounds may photobleach.[7] Since both compounds have similar line shapes between 1450 and 1550 cm^{-1}, only one was used in the fit to determine peak areas.

RESULTS

Freeze-Thaw Study. In the samples that were frozen and thawed to room temperature for longer than 10 min (Condition 1), the measured spectra showed noticeable decreases in signal at 1337 cm^{-1} and 1485 cm^{-1} (Fig. 1). These signals decreased to a minimum value within ~40 min and seemed to correspond to a decrease in the adenine contribution. The adenine signal could originate from many possible compounds containing adenine, such as adenosine, NADH, ATP, ADP, AMP, and FAD, which all have very similar spectra.[2] The signal remaining after 40 min at 1337 cm^{-1} and 1485 cm^{-1} was probably due to GMP. These spectral changes were reproducible and were observed for 7 pieces of colon tissue from 5 different patients. Detailed analysis of the spectra versus time was performed on a subset of these samples as listed in Table I. Quantitative spectral analysis showed that the relative adenosine level decreased monotonically with time while the guanosine contribution remained constant (Fig. 2), in agreement with the qualitative spectral changes noted in Fig. 1. The data in Fig. 2A also showed that the adenosine decrease is slower at 0–4 °C (filled circles) than at room temperature (open circles). As shown in Fig. 2A, 40 min after thawing to room temperature, the level of adenosine decreased to 50–30% of its original value, while it only reached 80% of its original value if the sample was kept refrigerated at 0–4 °C. The remaining biochemical compounds used in the linear model showed no monotonic changes during the testing period (not shown). For the samples that were thawed after freezing (Figs. 1 and 2), time t = 0 represents the moment the

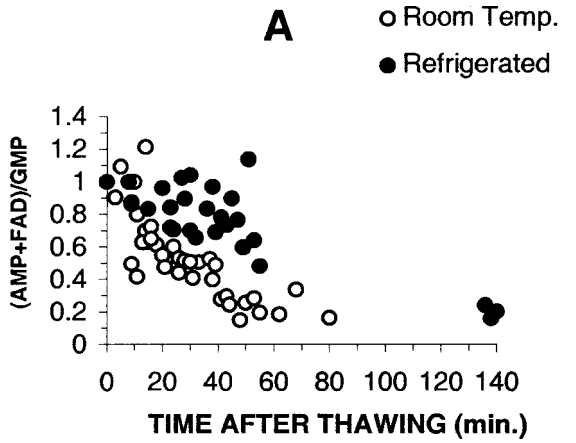

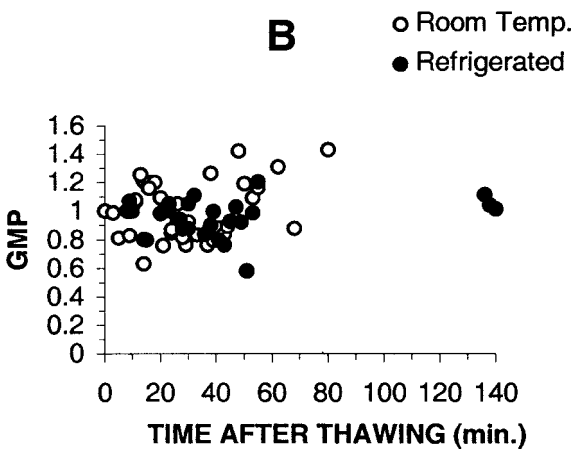

FIG. 2. Changes in adenosine (**A**) and guanosine (**B**) levels after thawing to room temperature or 0–4 °C. For samples tested after freezing and thawing (Condition 1) the level of adenosine (fit parameter $(a_{AMP} + a_{FAD})/a_{GMP}$) decreased monotonically while the guanosine level (fit parameter a_{GMP}) remained constant. The decrease in adenosine was slower for the samples kept refrigerated compared to those thawed to room temperature. Time t = 0 represents the moment the sample reached the desired thaw temperature (room temperature or 4 °C), as measured by a thermocouple near the mucosal surface. The fit parameters were obtained after fitting each UVRR spectrum to a linear combination of 10 line shapes (AMP, FAD, GMP, CMP, TMP, UMP, tryptophan, tyrosine, lipid, and water) by least-squares minimization as described previously.[2] For each sample tested, the levels of adenosine and guanosine were normalized to the value obtained at the earliest measured timepoint. The average initial values were 2.18 ± 0.45 for $(a_{AMP} + a_{FAD})/a_{GMP}$, and 0.018 ± 0.005 for a_{GMP} (mean of all samples tested ± standard deviation).

sample reached the desired thaw temperature (room temperature or 4 °C), as measured by a thermocouple near the mucosal surface. In Fig. 2, the adenosine and guanosine values were normalized to the values measured at the earliest available time point. Thus, the relative adenosine level was normalized to that within 10 min of thawing or to the level before freezing when available. The level of guanosine was always normalized to that within 10 min of thawing except for one case where the value obtained 23 min after thawing was used. The average initial values were 2.18 ± 0.45 for $(a_{AMP} + a_{FAD})/a_{GMP}$, and 0.018 ± 0.005 for a_{GMP} (mean of all samples tested (Table I) ± standard deviation).

In the samples that were not frozen (Condition 2), there

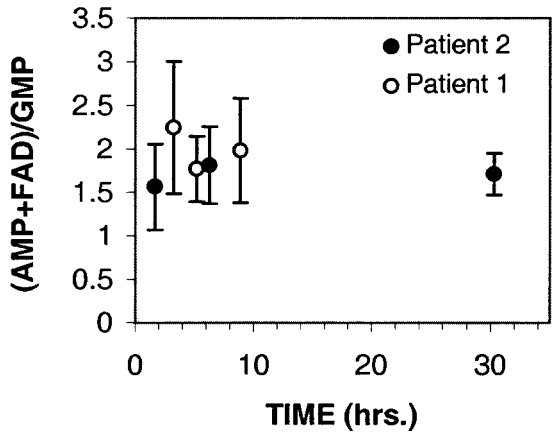

FIG. 3. Adenosine level for samples tested without freezing. The average level of adenosine remained constant for up to at least 30 h after surgical resection for colon samples tested without freezing (Condition 2). Data are shown for two colon samples taken from two different patients, and the error bars represent the standard deviation of the mean. The mean was obtained by averaging a set of measurements obtained by collecting a number of spectra from different locations on the mucosa (the number of locations tested varied between 5 and 11).

were no spectral changes, and the relative level of adenosine remained constant up to 30 h after surgical resection (Fig. 3). Although the data showed significant variation within each specimen, the average adenosine level remained constant and no monotonic changes were observed. For these samples, which were tested in Condition 2, the initial one-hour period immediately after devascularization was difficult to quantify with human samples, as intra-operative procedure time is variable. However, the rat colon, which was found to yield spectra similar to those of human colon, was used as a representative model. Thus, in a separate experiment done on rat colon tissue, the level of adenosine in mucosal spectra was shown to remain constant over a period that included the first hour after resection (data not shown).

It is also important to note that since the samples tested in Condition 2 (no freezing) did not show any spectral changes, the decrease in adenosine observed for the samples tested in Condition 1 (freeze/thaw) could be directly correlated to the effect of freezing and thawing on the colon specimens. In particular, the changes observed in Fig. 2 were not caused by the laser radiation. We also tested this hypothesis directly by testing a specimen after thawing it to room temperature and testing half of it immediately in the UVRR setup while the other half was kept in the dark at room temperature. Spectroscopy was subsequently done on the second half, about 30 min from thawing time. The level of adenosine measured in the second half, kept in the dark, was as low as that obtained at the end of testing the first half. This low level was 30% of the original level measured in the first spectra collected from the first half, tested immediately after thawing.

For the sample tested before freezing and within 5 min of thawing (Condition 3), the level of adenosine immediately after thawing was the same as that just before freezing (Fig. 4). This suggests that no change in adenosine content took place during the frozen phase.

Photobleaching. The photobleaching rate of UVRR colon spectra depended on several experimental param-

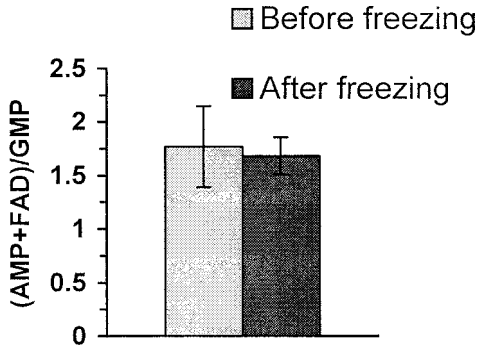

FIG. 4. Comparison between adenosine level before freezing and immediately after thawing. The level of adenosine immediately after thawing was the same as that before freezing (Condition 3). These data were collected from the same specimen, and the error bars represent the standard deviation of the mean. The mean was obtained by averaging a set of measurements taken from different locations on this specimen (n = 10 ''before freezing'', n = 4 ''after freezing'').

eters. Data collected from bulk specimens are shown in Fig. 5. Figure 5A shows how spectra of room-temperature colon samples changed as the fluence increased. The purine bands centered at 1337, 1485, and 1585 cm^{-1} decreased, and the tryptophan/tyrosine bands centered at ~1610 cm^{-1} increased and broadened. As shown in Fig. 5B, photobleaching effects can be slowed significantly by cooling the sample to 2–3 °C. For these spectra, a much larger energy dose was delivered to the sample, but photobleaching effects were considerably smaller. By bathing the sample in an argon gas atmosphere, there was little reduction in the 1485 cm^{-1} purine band (Fig. 5C), but spectral distortions in other areas of the spectrum were still present.

To quantify these effects, we plotted the time-integrated magnitude of the purine band at 1485 cm^{-1} as a function of fluence (Fig. 6). If no photobleaching occurrs, the time-integrated signal should increase linearly with delivered dose without saturating (solid line). As shown in the figure, the purine signal saturates very quickly at room temperature (circles) for fluences as low as 0.04 $mJ/\mu m^2$. The purine band's photobleaching was greatly slowed by cooling the samples or enclosing them in an argon atmosphere, as seen qualitatively in Fig. 5. For cooled samples (squares), we observed little signal saturation for fluences up to 0.3 $mJ/\mu m^2$ (2.13 mW delivered to a 35 × 40 μm^2 spot in 200 s). In argon (triangles) the purine signal stayed linear as fluence was increased to at least 0.35 $mJ/\mu m^2$. The solid line in Fig. 6 was obtained by a linear fit to the initial argon data from $\phi = 0.001$ to $\phi = 0.045$ $mJ/\mu m^2$.

DISCUSSION

Freeze-Thaw Study. The studies discussed were designed to investigate three issues: the stability of the UVRR spectrum over the test period, the effect of freezing and thawing on the spectra, and the extent of the period during which samples could be kept after surgical resection while still yielding reproducible spectra. Our studies show that freezing and thawing of the colon specimens results in a biochemical change manifested by a decrease in the adenosine UVRR scattering signal at 1337 cm^{-1} and 1485 cm^{-1}. This change can be slowed by keeping the samples refrigerated after thawing or can be avoided by not freezing the tissue samples. As long as the samples are not frozen, they can be used for UVRR spectroscopy if stored at 0–4 °C, up to 30 h after surgical resection. Our studies have also shown that the level of adenosine immediately after thawing is equal to that before freezing, suggesting that freezing by itself does not result in UVRR-detectable changes in adenosine content. However, although the effect of biodegradation on the UVRR spectra was addressed in this study, the results raise questions about the metabolic changes resulting from freezing and thawing and the molecules involved in that process. Further work, beyond the scope of the present study, is necessary to identify fully the specific adenylates associated with the change in adenosine Raman signal.

Cellular injury induced by surgical resection involves modes of damage related to ischemia following removal of the vascular supply and progressive loss of tissue integrity. Tissue freezing and thawing at high cooling rates (~200 °C/min for snap-freezing in liquid nitrogen) results in cell death, most probably due to intracellular ice formation.[8] In fact, to insure cell death, high cooling rates (25 °C/min) are clinically used during cryosurgery of diseased tissue.[9]

In the initial ischemic state after surgical resection, the colon studies showed no change in adenosine signal for up to 30 h (Fig. 3). Although the consumption of ATP is a well known effect of ischemia,[10–12] ATP depletion will not necessarily result in a decrease in adenosine UVRR signal (1337 cm^{-1} and 1485 cm^{-1} Raman bands) because byproducts of ATP degradation (ADP, AMP, adenosine, adenine) still contain the Raman-active adenyl moiety. Since our results showed no changes in adenosine UVRR signal, they suggest that no degradation beyond the level of adenine was taking place. This is consistent with a study on human myocardium collected from patients undergoing heart transplantation.[13] In that study, the hearts of 8 patients were stored in ice-cold Ringer's solution for up to 24 h. In that period, the level of ATP decreased to 58% of the pre-ischemic value, but the major fraction of catabolites remained nucleotides. The total amount of nucleotides (ATP + ADP + AMP) decreased by only 20%. These variables were species-dependent. In particular, in that same study, the total amount of nucleotides decreased to 63% of the pre-ischemic value in dog hearts. In our studies we found that spectra from unfrozen rat colon tissue behaved similarly to unfrozen human colon tissue (data not shown).

The effect of freezing and thawing, without cryoprotectants, on the metabolism of adenylates has not been studied as extensively as that of ischemia. Evidence of the activation of the ATP hydrolyzing enzyme by freezing has been previously observed,[14] and tissues that were frozen have shown ATP concentrations significantly lower than those before freezing, even when cryoprotectants were used.[15–17] While it is not clear how the presence of cryoprotectants directly affect these results, our data suggest that without cryoprotectants, ATP degradation evolves beyond the level of the nucleotides, as manifested by the decrease in adenyl signal in the UVRR spectra at 1337 cm^{-1} and 1485 cm^{-1}.

The studies presented here were designed to investi-

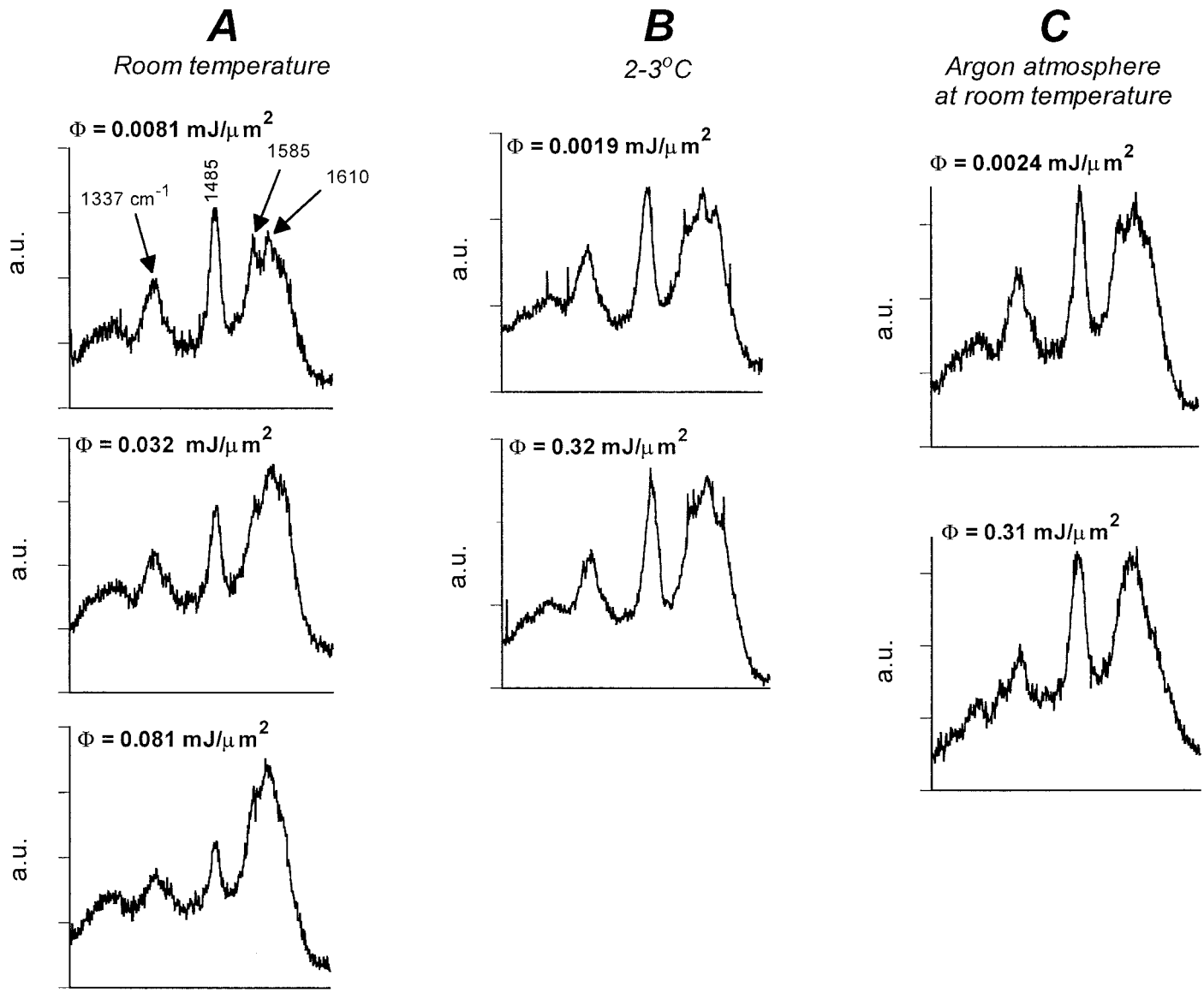

FIG. 5. Photobleaching of Raman spectra as a function of incident laser energy for samples tested in air at room temperature (**A**), in air at 2–3 °C (**B**), and at room temperature in an argon atmosphere (**C**). At room temperature (**A**), spectral changes due to photobleaching consist of a decrease in the purine signal (1337, 1485, 1585 cm^{-1}) and broadening and increase of the amino acid band around 1610 cm^{-1}. At room temperature (**A**), noticeable spectral changes are observed for a laser fluence, ϕ, as low as 0.03 $mJ/\mu m^2$, while at 2–3 °C (**B**) no changes are observed for up to at least 0.32 $mJ/\mu m^2$. In the argon atmosphere (**C**), the purine band decrease is avoided up to 0.31 $mJ/\mu m^2$, but other spectral distortions are still present. **a.u.** = arbitrary units representing the raw signal intensity collected from the CCD detector. Spectra in each column are plotted on the same scale.

gate the stability of the UVRR spectra and determine how unwanted biodegradation could be avoided. Although these studies do not provide specific information on the biochemical outcomes of freezing and thawing, they strongly suggest that UVRR spectroscopy could be used to non-invasively follow the depletion of the adenine nucleotide pool and possibly track cellular activity. While on-line Raman spectroscopy of adenine nucleotides has already been used in aqueous solutions,[18] the colon results discussed here suggest that it could be done in biological tissue.

Photobleaching. The effects of tissue temperature, oxygen, and laser power on photobleaching were investigated. Photobleaching manifested itself as a decrease in the purine bands (1337, 1485, and 1585 cm^{-1}) and an increase and broadening in the aromatic amino-acid bands (1610 cm^{-1}). In our study the pyrimidine signal could not be directly observed due to the smaller UVRR cross sections of the pyrimidines compared to the other compounds. As a result we have taken the photobleaching of the purines to be representative of general nucleotide photobleaching. The strength of the purine band was used as an indicator of photobleaching and was monitored as a function of fluence. The decrease in the strength of the purine band was slowed by cooling the tissue samples to 0–4 °C, or by placing the tissue in an argon atmosphere. On the other hand, the qualitative broadening of the aromatic amino acid band was not diminished by the argon atmosphere but was reduced by refrigerating the specimen during data acquisition. For cooled samples, we observed little purine photobleaching for fluences up to 0.3 $mJ/\mu m^2$ (2.13 mW delivered to a

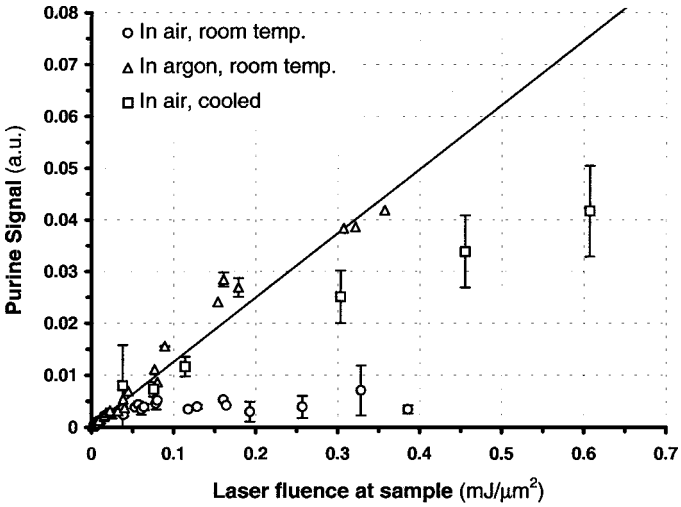

FIG. 6. Saturation of time-integrated purine Raman signal as a function of incident laser fluence at room temperature (circles), 2–3 °C (squares), and in argon (triangles). The purine signal was quantified by plotting the area of the 1485 cm^{-1} band. The band was fit to that of GMP at 1485 cm^{-1} and the baseline was fit to a constant. The fitting parameter for the GMP band represents the signal at 1485 cm^{-1} and is plotted here. The time-integrated signal was expected to increase linearly as a function of laser fluence in the absence of photobleaching (solid line). The data shown in this figure are consistent with those of Fig. 5. Namely, the signal saturates very quickly (at ~0.04 $mJ/\mu m^2$) at room temperature, while it increases linearly up to a laser fluence of 0.2 $mJ/\mu m^2$ under cooled conditions, and up to at least 0.35 $mJ/\mu m^2$ in argon. The solid line was obtained by a linear fit to the initial argon data from $\phi = 0.001$ to $\phi = 0.045$ $mJ/\mu m^2$. **a.u.** = arbitrary units.

35×40 μm^2 spot in 200 s). In a separate photobleaching study[19] conducted in microscopic tissue sections, we measured an exponential photobleaching rate, $\kappa = 0.572$ $(mJ/\mu m^2)^{-1}$, $1/\kappa = 1.75$ $mJ/\mu m^2$ for 12 μm thin sections. Thus, laser fluence levels under 0.2 $mJ/\mu m^2$ were necessary to collect spectra with minimal photobleaching from thin sections. We also found that the photobleaching rate, κ, was independent for power levels, if $P < 1$ mW. However, higher power levels resulted in a significantly higher photobleaching rate (κ approximately doubled for $P = 2.15$ mW). Finally, signal decrease due to photobleaching was decreased as tissue thickness increased. Accounting for the power levels and full tissue thicknesses used here, the data presented in this study corroborate our microscopic photobleaching data by showing a similar photobleaching rate.

The temperature and oxygen dependence of photobleaching observed in our study is consistent with the findings of other authors. In particular, our results suggest that tryptophan and tyrosine spectral changes are slowed by lowered temperature but not by the absence of oxygen in the environment. This is consistent with the finding that the formation of tyrosine and tryptophan radicals is enhanced by increasing temperature and can occur in both the absence and presence of oxygen[20,21] (even though the presence of oxygen may affect the formation of further byproducts). In the case of the purines, our data showed that purine signal decrease can be greatly slowed by replacing the air around the sample with argon gas. This was even effective at room temperature, suggesting that purely thermal damage is not sufficient to cause purine photobleaching. This also suggests that the purines in our system must be undergoing oxidative breakdown, which has been previously described and which relies on the presence of oxygen in the environment.[22] While pyrimidine photoproduct formation can be decreased by decreasing temperature,[7] the dependence of purine photobleaching on temperature is not well described in the literature. One possibility is that low temperature could reduce the rate of oxidative damage and in this way reduce photobleaching.

The incidence and type of protein and nucleotide photoproducts is likely to depend on the biochemical environment of the photobleaching species considered and the experimental conditions used. Thus, for instance, in the colon samples studied, nucleotides are not just present in double stranded DNA, but also in RNA, and in free form within the cytosol. This makes the biochemical analysis of photobleaching of nucleotides in the colon mucosa more complicated than analysis in pure double-stranded DNA. Nonetheless, studies in pure DNA or protein systems may give some indication of the potential photodamaging reactions that could occur within the colon mucosa. For example, in protein systems containing tyrosine and tryptophan, the principal products of UV-induced photochemical reactions are phenoxyl (from tyrosine) and tryptophanyl radicals, which can change further photochemically.[20,21,23–25] In peptide systems containing both tryptophan and tyrosine, the formation of tryptophanyl radicals may be a precursor to phenoxyl radical formation.[23]

The effect of 250 nm light on double-stranded DNA depends on the specific sequence of nucleotides comprising the DNA and the flexibility of the DNA at the photoproduct formation site.[26] The predominant photoproducts are pyrimidine derived and consist of cyclobutyl pyrimidine dimers and 6-4 pyrimidine adducts.[7] Other pyrimidine photoproducts, such as pyrimidine hydrates, may also form in lower yields.[27] Photochemical reactions of purines have also been identified.[22,26,28,29] Purine photoproducts could be the result of photochemical oxidation,[22] formation of covalent linkages between a purine and an adjacent base,[28] or photoinduced addition of a non-DNA compound, such as an amino acid, to a DNA base.[28,29] Although purines are believed to be more resistant to UV radiation than pyrimidines, depending on their position in the DNA base sequence purines may form photoproducts at moderate UV dosages and with yields comparable to those of pyrimidines.[26,30]

CONCLUSION

The results show that biochemical and photochemical artifacts can greatly affect the quality of the UVRR line shapes to be collected from biological tissues. The effects of both photo- and bio-degradation on the UVRR spectra of bulk colon tissue can be minimized by refrigerating the sample to 0–4 °C during data acquisition and keeping the laser fluence under 0.2 $mJ/\mu m^2$. Sample storage could be achieved by either refrigerating the specimens after surgical resection, without freezing, for up to at least 30 h, or snap-freezing in liquid nitrogen until use. However, when subsequently tested, the frozen and thawed samples could only be tested for a period of up to 30 min. These

findings can guide future ultraviolet spectroscopy studies of biological tissues.

ACKNOWLEDGMENTS

This work was conducted at the Massachusetts Institute of Technology Biomedical Research Center, supported by NIH-P41-RR02594. Additional support was provided by NIH RO1-CA53717 and NSF-9304251.

1. Y. Yazdi, N. Ramanujam, R. Lotan, M. Follen Mitchell, W. Hittelman, and R. Richards-Kortum, Appl. Spectrosc. **53,** 82 (1999).
2. N. N. Boustany, J. M. Crawford, R. Manoharan, R. R. Dasari, and M. S. Feld, Lab. Invest. **79,** 1201 (1999).
3. N. N. Boustany, R. Manoharan, R. R. Dasari, and M. S. Feld, Appl. Spectrosc. **54,** 24 (2000).
4. D. Strommen and K. Nakamoto, *Laboratory Raman Spectroscopy* (John Wiley and Sons, New York, 1984), pp. 115, 118.
5. G. Dellepiane and J. Overend, Spectrochim. Acta **22,** 593 (1966).
6. S. T. Wollman and P. W. Bohn, Appl. Spectrosc. **47,** 125 (1993).
7. M. H. Patrick and R. O. Rahn, ''Photochemistry of DNA and Polynucleotides: Photoproducts'', in *Photochemistry and Photobiology of Nucleic Acids,* Volume II, S. Y. Wang, Ed. (Academic Press, New York, N.Y., 1976).
8. P. Mazur, Science **168,** 939, (1970).
9. K. Tatsutani, B. Rubinsky, G. Onik, and R. Dahiya, Urology **48,** 441 (1996).
10. R. S. Cotran, V. Kumar, and S. L. Robbins, *Pathologic Basis of Disease* (W. B. Saunders Company, Philadelphia, 1989), 4th ed., pp. 2–12.
11. S. P. Andreoli, J. Lab. Clin. Med. **122,** 232 (1993).
12. F. Lang, G. L. Busch, and E. Gulbins, Nephrology, Dialysis, Transplantation **10,** 1551 (1995).
13. M. Masuda, S. Sukehiro, T. Mollhoff, H. R. Lu, H. Van Belle, and W. Flameng, J. Thorasic and Cardiovascular Surgery **103,** 993 (1992 May).
14. O. Scharff and B. Vestergaard-Bogind, Scandinavian J. Clin. Lab. Invest. **18,** 87 (1966).
15. E. Bosman, D. du Toit, P. H. Wessels, M. S. Bornman, and D. J. du Plessis, Arch. Andrology **33,** 7 (1994).
16. E. A. McLaughlin, W. C. L. Ford, and M. G. R. Hull, Int. J. Andrology **17,** 19 (1994).
17. S. A. Carney, M. Hall, and C. R. Ricketts, British J. Dermatology **87,** 23 (1972).
18. P. A. Walker III., W. K. Kowalchyk, and M. D. Morris, Anal. Chem. **67,** 4255 (1995).
19. N. Boustany, Ph.D. Thesis, Harvard-M.I.T. Division of Health Sciences and Technology (1997), Chap. 3, pp. 56–83.
20. D. Creed, Photochem. Photobiol. **39,** 537 (1984).
21. D. Creed, Photochem. Photobiol. **39,** 563 (1984).
22. D. Elad, ''Photoproducts of Purines'' in *Photochemistry and Photobiology of Nucleic Acids,* Vol. I, S. Y. Wang, Ed. (Academic Press, New York, 1976).
23. R. W. Sloper and E. J. Land, Photochem. Photobiol. **32,** 687 (1980).
24. M. Bazin, L. K. Patterson, and R. Santus, J. Phys. Chem. **87,** 189 (1983).
25. B. Finnstrom, F. Tfibel, and L. Lindqvist, Chem. Phys. Lett. **71,** 312 (1980).
26. M. M. Becker and Z. Wang, J. Mol. Biol. **210,** 429 (1989).
27. I. E. Kochevar and L. A. Buckley, Photochem. Photobiol. **51,** 527 (1990).
28. N. J. Duker and P. E. Gallagher, Photochem. Photobiol. **48,** 35 (1988).
29. K. C. Smith, ''The Radiation-Induced addition of Proteins and Other Molecules to Nucleic Acids'', in *Photochemistry and Photobiology of Nucleic Acids,* Vol. II, S. Y. Wang, Ed. (Academic Press, New York, 1976).
30. P. E. Gallagher and N. J. Duker, Photochem. Photobiol. **49,** 599 (1989).